JOURNAL OF SOLID STATE CHEMISTRY 32, 259–267 (1980)

Solid-State Electrochemical Studies of the Mixed Conductor $Cu_xMo_6S_{8-y}$. I. Partial Copper Ion Conductivity and Chemical Diffusion

G. J. DUDLEY,* K. Y. CHEUNG, AND B. C. H. STEELE

Wolfson Unit for Solid-State Ionics, Department of Metallurgy and Materials Science, Imperial College of Science and Technology, Prince Consort Road, London, SW7 2AZ United Kingdom

Received January 10, 1979; in final form May 11, 1979

The partial copper ion conductivity and chemical diffusion coefficient of the phase $Cu_xMo_6S_{8-y}$ ($y = 0.30 \pm 0.15$) have been determined as a function of x ($1.5 < x < 3.5$) and temperature ($396°K < T < 443°K$) from four-point dc polarization experiments. For a given temperature, both increased almost linearly as x was increased, $\tilde{D}$ at 441°K, for example, rising from 7×10^{-7} cm^2 sec^{-1} at $x = 1.5$ to 4.8×10^{-5} cm^2 sec^{-1} at $x = 3.37$. This behavior, together with the activation energy for conduction, is discussed in terms of the known arrangement of copper ion sites in the phase.

Introduction

Since their discovery (*1*) there has been much interest in phases of the general formula $M_xMo_6S_8$ primarily on account of their electronic superconducting properties. M can be one of a large number of metals and the range of x values for which compounds can be prepared varies from almost nil in the case of $Pb_xMo_6S_8$ to between 1 and 4 in the case of $Cu_xMo_6S_8$. In addition the Mo : S ratio can vary over small limits (*2*). It has been shown that for some metals (e.g., Cu, Ni, Fe) x can be reduced to zero by treatment of the powder with HCl (*3*), leaving the isostructural, but thermally unstable, phase Mo_6S_8. This indication of the high mobility of M was confirmed by Schöllhorn *et al.* (*4*) who changed x electrochemically in aqueous solution and furthermore demonstrated that in organic liquid electrolytes, alkali metals can be introduced into the structure.

The structure is based on Mo_6S_8 building blocks which are approximately cubic in shape. These are stacked in three dimensions in such a way that sulfur atoms from one cube lie near the face centers of adjacent cubes, leading to a rhombohedral symmetry, space group $R\bar{3}$ (*5*). The M sites lie nominally at the center of a large hole formed by a cube of sulfur atoms, one from each of the surrounding Mo_6S_8 groups. In the case of $M = Cu$, however, the cube is compressed along the threefold axis such that two sets of six equivalent tetrahedrally coordinated sites result, as shown in Fig. 1. These two sets of sites are shown in more detail in Fig. 6, where they are viewed along the threefold axis. The inner ones, Cu(A), are coplanar while the outer set, Cu(B), are alternatively above and below this plane. Each Cu(B) site lies quite close to another Cu(B) site (Cu(B)′) from the next group. Distances are shown in Fig. 6 for

* To whom correspondence should be addressed. Present address: Berec Group Ltd., Advanced Projects Group, 18, Nuffield Way, Ashville Trading Estate, Abingdon, Oxon, OX14 1TG, United Kingdom.

0022-4596/80/060259-09$02.00/0

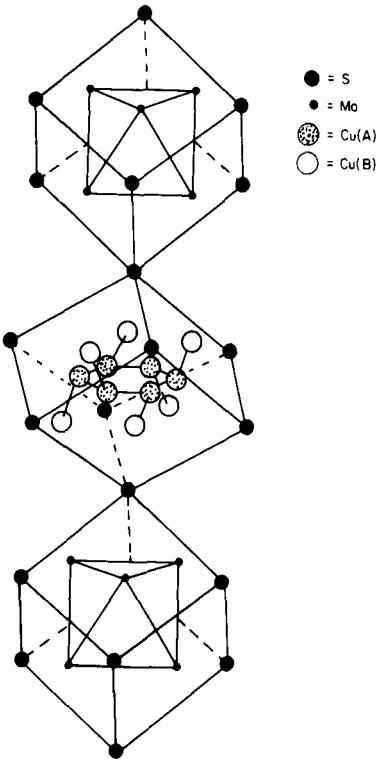

FIG. 1. Structure of $Cu_xMo_6S_8$. Reproduced, with permission, from Yvon (*5*).

the composition $Cu_{2.76}Mo_6S_8$ (*5*). These are quite sensitive to the value of x; increasing x leads to an increase in the Cu(*A*)–Cu(*B*) distance but to a decrease in the Cu(*B*)–Cu(*B*)′ distance. A three-dimensional network of pathways is thus formed along which Cu^+ ions can move. Being also a metallic conductor the compound fulfills the main requirements of a solid solution electrode (*6*), but differs from the majority of solid solution electrode materials so far studied in being a three-dimensional ionic conductor.

In the present work two kinetic transport properties of $Cu_xMo_6S_{7.59}$ have been measured as a function of x and temperature using a solid-state four-point conductivity cell of the type previously used by the authors in the systems $K_{1+x}Fe_{11}O_{17}$ (*7*) and $LiFe_5O_8$ (*9*). These are the partial ionic conductivity of Cu^+ ions (σ_i) and the chemical diffusion coefficient $\tilde{D}$ characterizing motion of copper ions and electrons, coupled by the requirement of local charge neutrality (ambipolar diffusion). The equilibrium cell emf variations with composition and temperature, obtained along with the transport data, are reported in the accompanying paper (*10*).

Experimental

Preparation of Materials

$Cu_2Mo_6S_{7.59}$ was prepared by direct reaction of molybdenum powder (99.99% Koch–Light), copper powder (99.3%, Koch-Light), and sulfur (Specpure, Johnson-Matthey) in a silica tube sealed under vacuum. It was heated to 1275°K for 2 days 1375°K for 3 hr, and then quenched in air The resulting powder was finely ground and cold-pressed into 8-mm-diameter pellets These were stacked together, wrapped in 0.025-mm-thick platinum foil and hot-pressed in a 12.5-mm-diameter graphite die filled with boron nitride powder as the pressure transmitting medium. The pellets, pressed at 1600°K for 2 hr at 5×10^7 N m^{-2}, attained a density of 5.69 g cm^{-3} (98.4% theoretical using measured lattice parameters and assuming the nonideality of the Mo:S ratio to be due to S vacancies). Sulfur loss was minimized by the encapsulation technique X-Ray powder photographs of the material as prepared showed no impurity phases However, at a later stage, using samples that had had their copper content increased electrochemically, the molybdenum metal 110 line became visible. This had been obscured in the original sample by the 131 line of $Cu_2Mo_6S_8$. The phase limits for $Cu_2Mo_6S_{8-y}$ have since been determined as $0.15 < y < 0.30$ (*2*) and we conclude that the actual starting composition of the sample used in this work may be more accurately represented as $Cu_{2.03}Mo_6S_{7.7}+0.09$Mo (metal). We

would not, however, expect that the Mo:S ratio could change during electrochemical alteration of the copper content because of the low temperatures involved compared to those used in the initial preparation. It is also possible that the phase limits of the copper Chevrel phase correspond not to a deficiency of sulfur but to an excess of molybdenum, in which case the composition of the sample used in this work would be $Cu_{2.11}Mo_{6.23}S_8 + 0.09Mo$. A similar uncertainty exists in the case of $Pb_{0.92}Mo_6S_{7.5}$ (*2*, and references cited therein). Because of this we have retained the 'as-prepared' formula $Cu_2Mo_6S_{7.59}$ as the starting composition from which the subsequent copper contents (x) were calculated.

The copper ion electrolyte was CuBr + 1,4-dimethyl-1,4-diazabicyclo-2,2,2-octane dibromide in a mole ratio of 94:6 as described by Takahashi *et al.* (*11*). The preparation was essentially as reported by Armstrong *et al.* (*12*) except that the resulting powder was hot-pressed at 443°K for 20 hr at a pressure of 6×10^7 N m^{-2} to give a dense material. Hebb–Wagner polarization measurements indicated that the electronic conductivity at 414°K was in the region of $10^{-11}\ \Omega^{-1}\ cm^{-1}$ (*13*), so that electronic leakage did not have to be taken into account in the present work.

$Cu_{1.75}S$ was prepared from the elements in a sealed silica tube, ground, and hot-pressed under vacuum in a graphite die at 1225°K under 3×10^{-7} N m^{-2} pressure for 2 hr (*13*).

All cell components except for the electrolyte were machined using an oil-lubricated annular diamond saw. The electrolyte was ground manually in a dry glove manipulator box because of its sensitivity to air and water vapor which can lead to increased electronic conductivity.

Cell Configuration

The conductivity jig, illustrated in Fig. 2, differed slightly from that used previously (*7*, *9*). The sample was a bar of dimensions $5.7 \times 1.2 \times 1.3$ mm at the ends of which were pressed 1-mm-thick slices of the electrolyte, in turn contacted by the pieces of $Cu_{1.75}S$ acting as reservoirs of copper ions. Electrical contact was made by means of platinum foil and the whole assembly was clamped in a miniature stainless-steel G-clamp with a tungsten compression spring. This assembly rested between the ionic and electronic

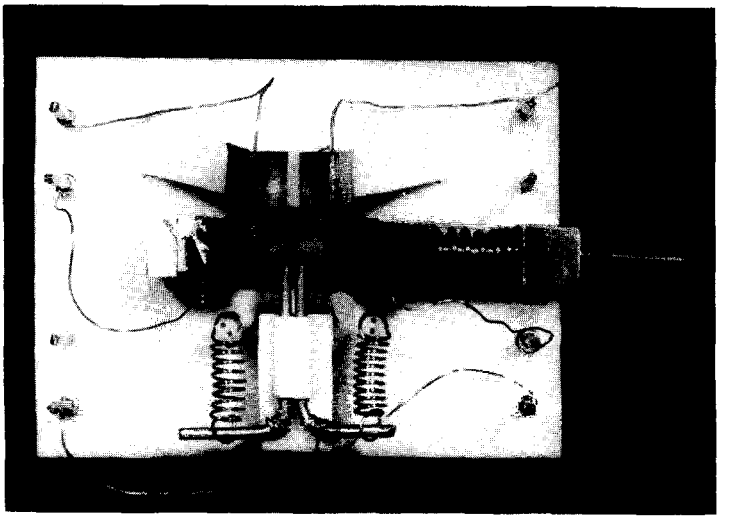

FIG. 2. View of cell for four-point ionic conductivity and diffusion measurements.

voltage probes, of which the former were made from pieces of electrolyte ground to the desired shape in an inert atmosphere glove box. Copper metal was vacuum deposited on the outermost sides of the ionic probes to produce copper reference electrodes. Wires from the cell contacts were wire-wrapped onto a set of square-section platinum–10% rhodium contact posts. This is the stage shown in Fig. 2. This whole unit was placed on a larger horizontal flat alumina holder also equipped with contact posts adjacent to the first set. The contacts on the holder were permanently connected by platinum–rhodium wire which led outside the apparatus. The unit in Fig. 2 was connected to the holder by wire-wrapping between adjacent contact posts and the completed cell placed inside a glass envelope itself inside a horizontal tube furnace. The atmosphere surrounding the assembly was argon which had been dried and passed over titanium at 750°C.

Voltages were measured by a Data-Precision 3500 digital voltmeter which was coupled to a Commodore P.E.T. 2001-8 microcomputer via an interface unit constructed in the laboratory. This interface also allowed the computer to select any one of ten voltage sources to be measured, to control the constant current source and the temperature of the cell. A control program enabled complete four-point conductivity experiments to be carried out automatically and the chemical diffusion coefficients to be calculated. The steady-state probe voltages were taken to have been reached when a least-squares regression of the last 20 readings had a slope of less than 8 μV/hr. The ionic conductivity configuration is shown in Fig. 3a. The voltage between the current contacts, V3, was not allowed to exceed 50 mV. Reed switches controlled by the computer also allowed the connections to the cell to be changed for coulometric titrations, as shown in Fig. 3b. This enabled the copper content of the sample to be changed *in situ* by

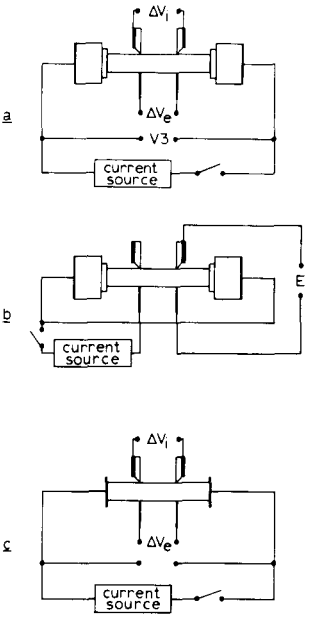

FIG. 3. Cell configurations used. (a) Four-point ionic conductivity; (b) coulometric titration; (c) four-point electronic conductivity.

the passage of a constant current for a known time. Once the new concentration was constant throughout the bar, indicated by a stable value of the cell emf E, the ionic conductivity mode could be reselected ready for measurements as a function of temperature at the new composition. Details of the computer-controlled system will appear elsewhere.

Results and Discussion

Principle of the Measurements

For details the reader is referred to Refs. (*7*, *8*). Only a brief summary follows below. The ionic conductivity measurement is an ionic analog of a four-point electronic measurement. After a constant current of copper ions has been flowing through the bar for a long time, all electronic motion has been stopped by the electronically blocking electrolyte; hence a partial ionic conductivity σ_i can be calculated from the ionic probe

voltage difference, ΔV_i, and the specimen geometry. This conductivity may differ slightly from the total conductivity multiplied by the transport number for ions if Onsager cross-coefficients are significant (*7*, *14*). We show later, however, that these are in fact very small. In contrast to samples with only one conducting species, when the steady ionic probe voltage difference is obtained immediately upon switching on the constant current, in a mixed conductor this state is reached slowly via a diffusion process. From analysis of the variation of the ionic probe voltage with time it is possible to calculate the chemical diffusion coefficient for the system (*15*). Specifically for long times the probe voltage varies according to an exponential law and a time constant τ can be defined, which is related to the chemical diffusion coefficient by $\tilde{D} = Z^2/\pi^2\tau$, where Z is the length of the bar sample. An example of the behavior of the probes during passage of an ionic current is shown in Fig. 4. No changes were observable in the electronic probe voltages because of the much larger electronic conductivity.

Ionic Conductivity Results

These are shown as a function of x in Fig. 5, together with the activation energy E_a calculated from the relation

$$\sigma T = \sigma_0 \exp(-E_a/RT).$$

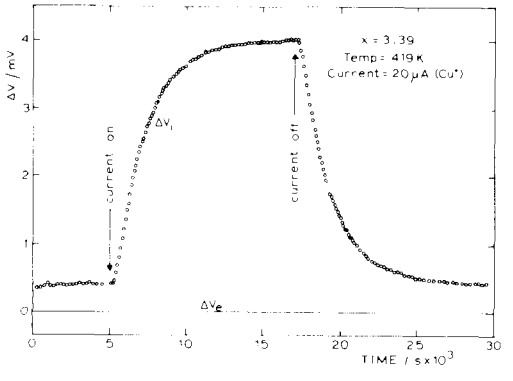

FIG. 4. Behavior of voltage probes as a function of time on switching on and off a current of Cu^+ ions.

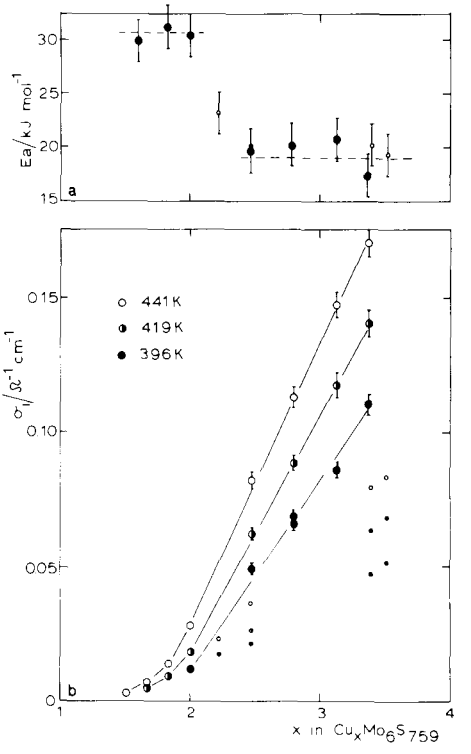

FIG. 5. (a) Energy of activation for ionic conduction as a function of x. (b) Partial ionic conductivity of $Cu_xMo_6S_{7.59}$ as a function of x and temperature. Smaller circles show results from second cycle.

The error bars in σ_i indicate the estimated uncertainties due to fluctuations in the measured ionic probe voltage and to the limited accuracy of the measurement of the probe spacing. Error bars in E_a were obtained by taking worst-case combinations of the errors in the individual σ_i values. The conductivities are very close to straight-line functions of x for $2 < x < 3.4$ and the activation energy for conduction remains fairly constant at 19 kJ $mole^{-1}$. This suggests that there is a fairly constant mobility and the ionic conductivity in this region is proportional to the number of occupied Cu(B) sites, as expected when there is an excess of empty sites. At lower values of x the activation energy rises some 50% and the conductivity deviates from a straight line. Extrapolations of the straight parts cross the x axis at about

$x = 1.8$. This suggests that there are two types of site for copper ions: that of lower energy is associated with a low mobility while above $x = 1.8$, the higher-energy sites begin to be filled and these are associated with a high mobility. It is natural to choose the Cu(A) and Cu(B) sites as the two sites involved but it is not obvious from simple structural considerations why either set should be filled at $x = 1.8$. The sites are shown looking down the threefold axis in Fig. 6 (*15*). Since the radius of a Cu^+ ion (0.96 Å) is greater than half the separation between the Cu(A) sites, a maximum of 3 Cu^+ ions might be expected to occupy these sites rather than 1.8. However Yvon and collaborators have derived values for the room-temperature occupancies of these sites from X-ray diffraction data. These are also shown in Fig. 6. This additional experimental evidence thus supports the conclusion tha the Cu(A) sites do indeed have a maximun occupancy of about 1.8.

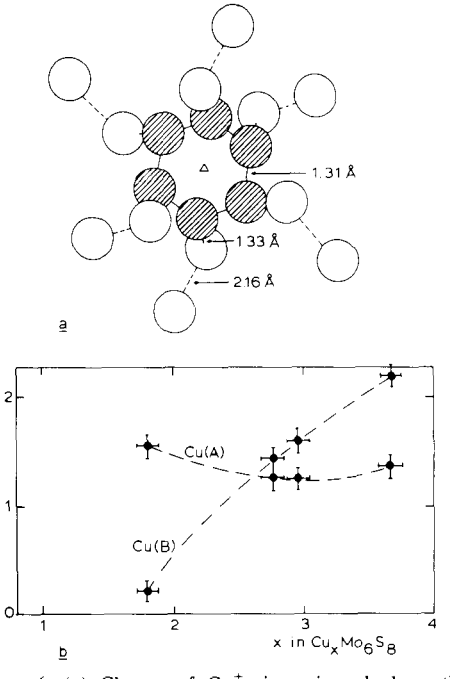

FIG. 6. (a) Cluster of Cu^+ sites viewed along the threefold axis. Cu(A) sites are shown shaded, Cu(B) unshaded. The outer Cu(B) sites belong to adjacent clusters. (b) Occupancy of Cu(A) and Cu(B) sites at room temperature as a function of x. Both (a) and (b) are reproduced, with permission, from Yvon *et al.* (*16*).

Chemical Diffusion Results

These are shown in Fig. 7. In contrast tc the conductivity results two values of $\tilde{D}$ are obtained in each experiment, one from the behavior of the ionic probe voltage difference after current switch-on and the other after current switch-off. Both values are shown and the error bars indicate the estimated effects of uncertainties in the steady-state ionic probe voltage difference ΔV_i. In an earlier paper (*7*) it was shown that the chemical diffusion coefficient could be related to the partial conductivities of ions (σ_i) and electrons (σ_e), the molar volume of the sample (M/ρ), and the slope of the equilibrium cell emf E as a function of x:

$$\tilde{D} = \frac{\sigma_i \sigma_e M}{(\sigma_i + \sigma_e) F \rho} \frac{dE}{dx}. \qquad (1)$$

For $\sigma_e \gg \sigma_i$, as in the present case,

$$\tilde{D} \sim \sigma_i \frac{M}{F\rho} \frac{dE}{dx}.$$

Neglecting changes in $M/F\rho$ it can be seen that the difference in shape between the $\tilde{D}$ versus x curve and the σ_i versus x curve is due to variations in the thermodynamic factor dE/dx. This has been calculated by drawing tangents to the graph of E versus x for this system reported in the accompanying paper (*10*), where E is the emf of the cell $Cu/electrolyte/Cu_xMo_6S_{7.59}$ obtained by measuring the voltage between ionic and electronic voltage probes when the bar is at equilibrium. Values of $\tilde{D}$ calculated from the probe voltage transient are compared to values calculated from the right-hand side of Eq. (1) in Fig. 8. The agreement is within experimental error, the largest contribution to which is the uncertainty in the value of dE/dx.

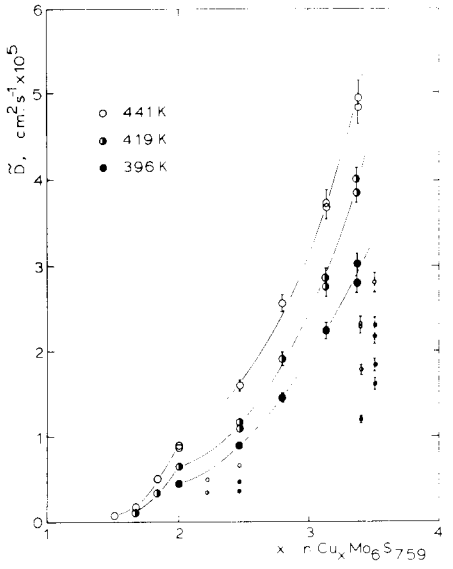

FIG. 7. Chemical diffusion coefficient $\tilde{D}$ of $Cu_xMo_6S_{7.59}$ as a function of x and temperature. Smaller circles show results from second cycle.

Changes in σ_i on Cycling

The nominal starting composition of the sample was $Cu_2Mo_6S_{7.59}$. x was increased to 3.4 and then decreased again. All measured quantities were in good agreement on the return part of the cycle with those measured as x was increased. x was then taken below 2. On returning from these low x values, however, both $\tilde{D}$ and σ_i had fallen to about one-half their values before, although the cell emf was still in close agreement (*10*). These values are shown in Figs. 5 and 7 by small circles. We interpret this as being due to the formation of small cracks in the polycrystalline sample due to the anisotropic changes in lattice parameters accompanying changes in x. These are most severe in the region $1.5 < x < 2.0$ (*2*).

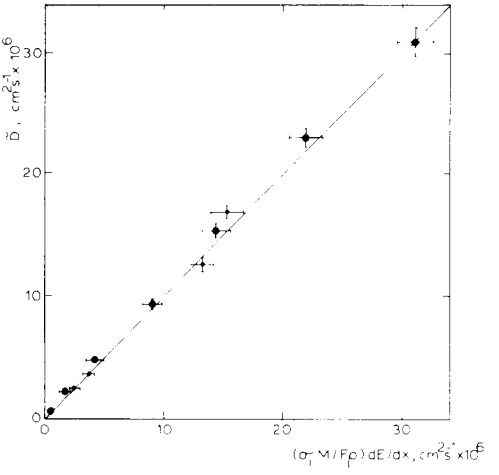

FIG. 8. Comparison of $\tilde{D}$ calculated from transients with that calculated from ionic conductivity, molar volume, and thermodynamic factor (Eq. (1)).

Electronic Conductivity and Cross-Coefficients

After completion of the partial ionic conductivity measurements, with the composition at $Cu_{3.39}Mo_6S_{7.59}$, the ionic current contacts were replaced with electronic contacts (platinum foil). Electronic currents were passed through the bar and the behavior of the voltage probes was monitored. An example is shown in Fig. 9, which is at the same composition and temperature as the ionic current experiment depicted in Fig. 4. Because of the large partial electronic conductivity, a large current was necessary and the changes in the probe voltages were rather small. Considering first the behavior of the electronic probes it was found that the partial electronic conductivity decreased with increase of temperature, as found by Flukiger *et al.* (*17*) for $Cu_{3.2}Mo_6S_8$. Our

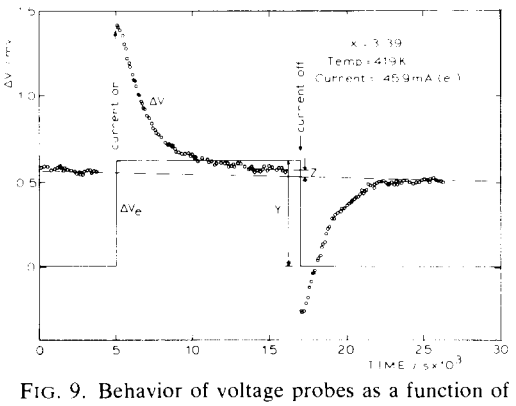

FIG. 9. Behavior of voltage probes as a function of time on switching on and off an electronic current.

values are about 50% lower than those obtained by extrapolation of their data, which is about the same as the decrease in ionic conductivity of our specimen on going from the first to the second cycle. The individual data points are not shown for the electronic probes since the scatter was very small owing to the low resistance between these probes. On the other hand scatter in the ionic probe voltages was quite large which led to low precision in the values of $\tilde{D}$ calculated from the ionic probe transients. These nevertheless agreed to within 25% with those obtained in the ionic current experiments under the same conditions. At the instants of current switch-on and switch-off the ratio of the probe voltage change to the probe spacing should be identical for both types of probes. This was found to be the case within experimental error, the ratio $\Delta V_i/\Delta V_e$ being 1.400 and 1.375, respectively, compared to 1.431 for the ratio of probe spacings measured with a traveling microscope. It is of interest whether the presence of a vastly dominant electronic conductivity leads to nonzero values of the Onsager cross term L_{ie} in the flux equations. These read:

$$J_i = L_{ii}\nabla\bar{\mu}_i + L_{ie}\nabla\bar{\mu}_e,$$

$$J_e = L_{ee}\nabla\bar{\mu}_e + L_{ei}\nabla\bar{\mu}_i,$$

where $\bar{\mu}_e$ and $\bar{\mu}_i$ are the electrochemical potentials of electrons and Cu^+ ions. As was shown previously (*7*) the ratio L_{ie}/L_{ii} can be obtained from the negative value of the ratio of the gradient of electrochemical potential of ions to that of the electrons when an electronic current is passing and a steady state has been reached. Therefore in Fig. 9 it is given by the ratio of Z to Y, modified to take into account the difference in probe spacings. Over eight experiments at temperatures between 396 and 443°K, Z/Y ranged from -0.05 to -0.13. However Z was not much larger than the baseline scatter in ΔV_i and moreover such a small negative value could arise from insufficient time being allowed for the probe voltages to reach thei true steady-state values.

Electronic current experiments were no carried out at other compositions since cou lometric titrations were not possible with thi cell configuration.

Conclusions

The partial conductivity of copper ions ir $Cu_xMo_6S_{7.59}$ has been measured as a function of x and found to be high wher $x > 2$. Since the transport number of coppe ions is very small, typically 2×10^{-4}, the chemical diffusion coefficient of the ions anc electrons follows trends similar to those o the conductivity, but is modified by the thermodynamic factor dE/dX (sometime called the thermodynamic enhancemen factor (*18*)). The relation linking these three quantities (Eq. (1)) has been verified. The increase in the ionic conductivity above $x = 2$ can be explained by the assumption that the lowest-energy sites (Cu(A)) become fully occupied around this composition and above $x = 2$ higher-energy sites (Cu(B)) begin to be populated. These Cu(B) sites lie nearer tc the top of the energy barrier separating groups of sites in neighboring unit cells across which ions have to pass. The measured activation energies for ionic conduction support this view and indicate a difference in energy between the two types of site of about 13 kJ mole^{-1}.

The Onsager cross-coefficient L_{ie} governing possible coupling between ionic and electronic fluxes (other than by the common electric field) was found to be less than 8% of the main term L_{ii} at $x = 3.39$, and probably close to zero.

Acknowledgements

We thank Mr. C. Stewart for performing some o the electrochemical measurements, and acknowledge financial support from the Anglo-Danish E.E.C Project, Contract 316-78-EE.

References

1. R. CHEVREL, M. SERGENT, AND J. PRIGENT, *J. Solid State Chem.* **3**, 515 (1971).
2. K. Y. CHEUNG AND B. C. H. STEELE, to be published.
3. R. CHEVREL, M. SERGENT, AND J. PRIGENT, *Mater. Res. Bull.* **9**, 1487 (1974).
4. R. SCHÖLLHORN, M. KUMPERS, AND J. O. BESENHARD, *Mater. Res. Bull.* **12**, 781 (1977).
5. K. YVON, *Solid State Commun.* **25**, 327 (1978).
6. B. C. H. STEELE, *in* "Superionic Conductors," (G. D. Mahan and W. L. Roth, Eds.), pp. 47–65, Plenum, New York (1976).
7. G. J. DUDLEY AND B. C. H. STEELE, *J. Solid State Chem.* **21**, 1 (1977).
8. G. J. DUDLEY AND B. C. H. STEELE, *J. Solid State Chem.* **31**, 233 (1980).
9. G. J. DUDLEY AND B. C. H. STEELE, *J. Electrochem. Soc.* **125**, 1994 (1978).
10. G. J. DUDLEY, K. Y. CHEUNG, AND B. C. H. STEELE, *J. Solid State Chem.* **32**, 269 (1980).
11. T. TAKAHASHI, O. YAMAMOTO, AND S. IKEDA, *J. Electrochem. Soc.* **120**, 1431 (1973).
12. R. D. ARMSTRONG, T. DICKINSON, AND K. TAYLOR, *J. Electroanal. Chem.* **57**, 157 (1974).
13. J. M. SHEMILT, Ph.D. thesis, University of London (1978).
14. C. WAGNER, *Progr. Solid State Chem.* **10**, 3 (1975).
15. I. YOKOTA, *J. Phys. Soc. Japan* **16**, 2213 (1961).
16. K. YVON, A. PAOLI, R. FLÜKIGER, AND R. CHEVREL, *Acta Crystallogr. B* **33**, 3066 (1977).
17. R. FLUKIGER, A. JUNOD, R. BAILLIF, P. SPITZLI, A. TREYVAUD, A. PAOLI, H. DEVANTAY, AND J. MULLER, *Solid State Commun.* **23**, 699 (977).
18. W. WEPPNER AND R. A. HUGGINS, *J. Electrochem. Soc.* **124**, 1569 (1977).